

# A Jahn–Teller Geometric Distortion Effect on the Woodward–Hoffmann Rule in Thermal Decompositions of Diazetines

Shinichi Yamabe\*<sup>†</sup> and Tsutomu Minato<sup>‡</sup>

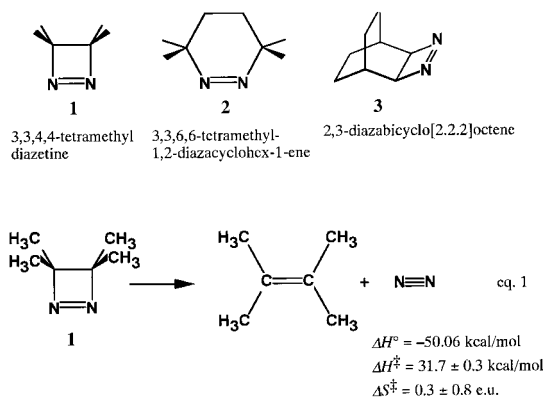
Department of Chemistry, Nara University of Education, Takabatake-cho, Nara 630-8528, Japan, and  
Institute for Natural Science, Nara University, 1500 Misasagi-cho, Nara 631-8502, Japan

Received: February 21, 2001; In Final Form: May 21, 2001

$N_2$  extrusion paths of the smallest monocyclic azoalkane, diazetine, its tetramethyl-substituted derivative, and their three-membered cyclic isomers were investigated by ab initio calculations. Systematic considerations of the orbital correlation diagram predicted that the routes conserving the  $C_s$  point group are symmetry allowed. CASSCF(2,2)/6-31G\*, CASSCF(4,4)/6-31G\*, and CASSCF(2,2)/6-311+G(2d,p) geometry optimizations were carried out and showed that the decomposition paths of the isomers followed the Woodward–Hoffmann rule. However, the paths of diazetines did not follow it. The dual orbital-mixing rule proposed here correctly explained the Jahn–Teller effect. Reaction enthalpy and activation energy were satisfactorily reproduced by the BCCD(T)/6-31G\*//CASSCF(2,2)/6-31G\* energies.

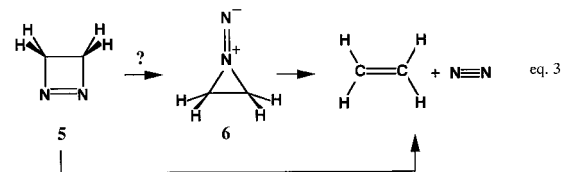
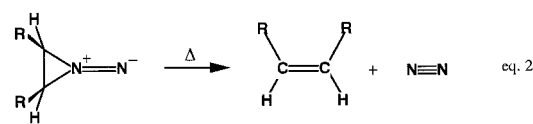
## I. Introduction

Cyclic and bicyclic azoalkanes (e.g., **1–3**) are known to be decomposed thermally and stereospecifically.<sup>1</sup> The simplest species **1** affords the olefin and nitrogen molecule in eq 1.<sup>2</sup>

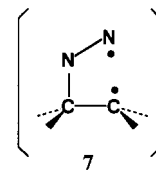


Although the reaction releases the large ring-strain instability of **1**, the observed activation energy,  $E_a = 32 \text{ kcal/mol}$ , is large. Despite accumulation of thermochemical and spectroscopic data of those azoalkanes, the mechanism of the nitrogen extrusion reactions is still unclear.

On the other hand, a three-membered intermediate was reported to undergo the  $N_2$  elimination stereospecifically (eq 2).<sup>3</sup> A decomposition path of the tetramethyl-substituted intermediate **4** is considered here. Parent species of **1** and **4** are structural isomers, **5** (diazetine) and **6** (eq 3), respectively. It is tempting to investigate  $N_2$  extrusion paths of **5** and **6** theoretically. Are those paths independent or dependent (**5**  $\rightarrow$  **6**  $\rightarrow$  ethylene +  $N_2$ )? The  $N_2$  elimination involves the homolytic cleavage of two C–N bonds of **5** and **6** and some biradical



species (e.g., **7**) might exist during the elimination. Geometries



of both **5** and **6** have the  $C_{2v}$  point group, and elimination paths may be controlled by the symmetry conservation (Woodward–Hoffmann, W–H) rule.<sup>4</sup>

Despite simplicity of the decomposed products in eq 3, no theoretical approaches to the reaction have been made so far. On the other hand, there are some computational studies of structural and electronic properties of diazetines<sup>5</sup> and their related azo compounds.<sup>6</sup> In this work, reaction paths of eqs 1 and 3 are investigated by the use of ab initio calculations. The following three problems are considered.

(1) Are those paths controlled by the W–H rule? Systematic analyses of the symmetry imposed on them are needed. (2) Is the isomerization route, **5**  $\rightarrow$  **6**, present or absent? (3) Do any biradical intermediates such as **7** intervene in the elimination?

<sup>†</sup> Department of Chemistry.

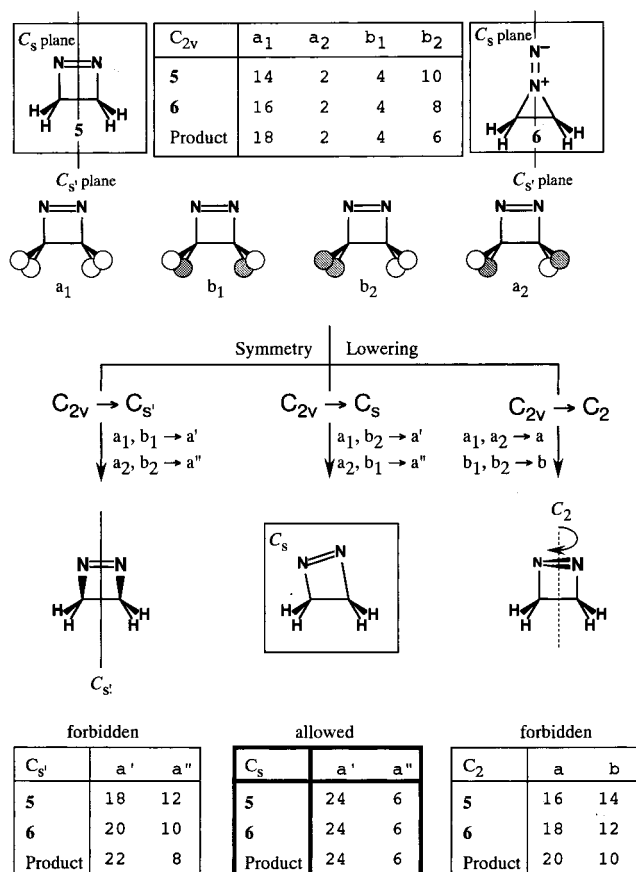
<sup>‡</sup> Institute for Natural Science.

It will be shown that the “least-motion path” regulated by the W–H rule is affected by the Jahn–Teller effect<sup>7</sup> through the orbital mixing. The W–H rule is based on the idea that reactions should proceed without needless geometric distortions and should take the least-motion path. In other words, the symmetry imposed on the system should be conserved during a reaction. When the electron assignment to respective irreducible representations in the reactant is different from that in the product, the reaction cannot take the least-motion path and is called “symmetry forbidden”. The Jahn–Teller effect states that in a high symmetric geometry two independent wave functions composed of different electron assignments may be degenerate and the geometry may be unstable. The symmetry relaxation leads to the energy lowering. Apparently, the effect is in conflict with the idea of the W–H rule. It is of theoretical interest to examine the effect in a “symmetry-allowed” path. Equations 1 and 3 will be investigated in this respect.

## II. Method of Calculations

As stated in Introduction, biradical intermediates might exist in reaction of eqs 1 and 3. Even without them, the biradical character is strong in transition states (TS) of those eliminations. Hartree–Fock and its perturbation methods are inapplicable to this work. Density functional theory (DFT)<sup>8</sup> methods were tested first. The hybrid functional B3LYP<sup>9</sup> was found to fail in determining the TS structure due to Hartree–Fock mixing. Second, pure DFT methods, BLYP<sup>10</sup> and B3PW91<sup>11</sup> were employed and were found to be also unsuccessful. Third, the completely active space SCF(CASSCF)<sup>12</sup> method was adopted for geometry optimizations.

CASSCF accounts for nondynamic electron correlations and was indeed found to be appropriate for the optimizations. CASSCF(2,2) and CASSCF(4,4) were used. The initial orbitals for CASSCF are the natural orbitals generated from the unrestricted Hartree–Fock wave functions. Energies must be evaluated including the dynamic electron correlations. CASPT2, which is a variant of CASSCF and includes Møller–Plesset perturbation theory,<sup>13</sup> was tested. But, the calculated results were unreasonable (e.g., negative activation energies). This is probably related to the fact that CASPT2 suffers from systematic errors either when the number of unpaired electrons changes along the reaction path<sup>14</sup> or when the system size is large and the size-consistency problem of “the CI ansatz”<sup>15</sup> becomes significant. Coupled-cluster theories utilize excitations from a Hartree–Fock wave function and account for a greater part of the total correlations energy.<sup>16</sup> But the solution of those theories may suffer from the instability in low-symmetry biradicals. Instead of the CCSD(T) approach, the Brueckner orbital based on coupled-cluster calculation,<sup>17</sup> Brueckner doubles with a triples contribution BCCD(T), is thought to give reliable single-point energies.<sup>18</sup> At the fifth order of perturbation, BCCD incorporates more terms than CCSD and QCISD. Thus, the BCCD(T)//CASSCF single-point calculations were carried out here. The basis sets used are mainly 6-31G(d) and 6-311+G(2d,p) for parent systems. Thermochemical data ( $\Delta H^\circ$  and  $\Delta S^\circ$ ) were obtained by the CASSCF(2,2)/6-31G\* vibrational analysis. In the enthalpy, the CASSCF(2,2)/6-31G\* electronic energies were replaced to the BCCD(T)/6-31G\* ones. The temperature was set to  $T = 420$  K, which is an average of experimental conditions.<sup>1</sup> All the calculations were performed by the use of the GAUSSIAN94 program package<sup>19</sup> installed both at the Compaq ES40 computer (The information Processing Center, Nara University of Education) and at the HP SPP1600 XA computer (Computer Center, Nara University).

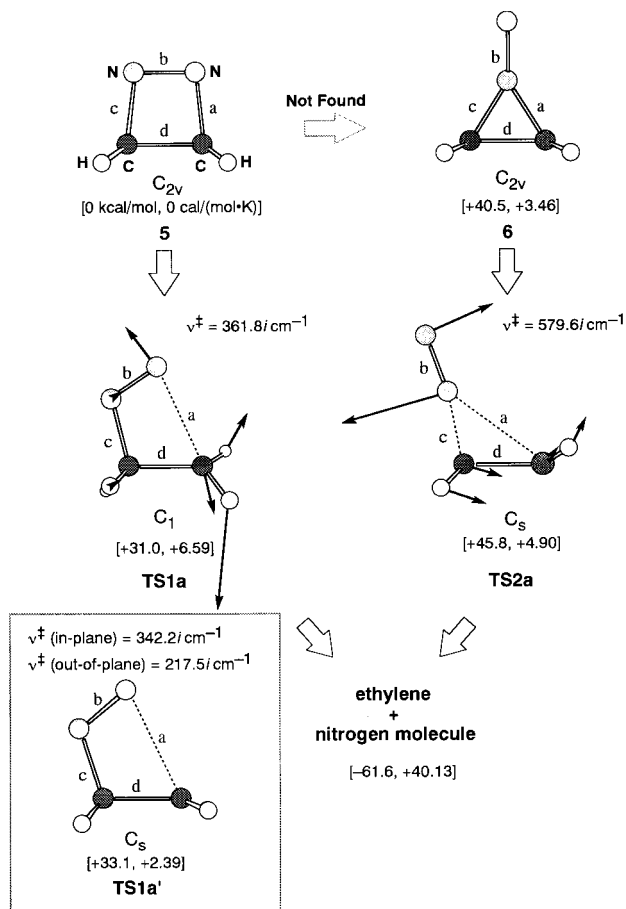


**Figure 1.** Electron assignment equivalent to orbital correlation diagram for the diazetine decomposition under the  $C_{2v}$  symmetry, and three symmetry relaxations and the resultant mixed electron assignment. “Product” is a ( $H_2C=CH_2$  and  $N_2$ ) system.

## III. Orbital Correlation Diagram

The parent diazetine **5** and its isomer **6** have geometries of  $C_{2v}$  point group. First, the orbital correlation diagram between **5** and the products (ethylene and  $N_2$ ) is drawn, and the resultant electron assignment is shown in Figure 1. Thirty electrons of the reacting systems **5** are classified as four irreducible representations:  $a_1$ , 14;  $a_2$ , 2;  $b_1$ , 4;  $b_2$ , 10, respectively. For the product, they are  $a_1$ , 18;  $a_2$ , 2;  $b_1$ , 4; and  $b_2$ , 6. The electron assignments are different between **5** and the product. The  $C_{2v}$  conserved path is, therefore, symmetry forbidden. Also, the  $C_{2v}$  path from **6** ( $a_1$ , 16;  $a_2$ , 2;  $b_1$ , 4;  $b_2$ , 8) to the product is forbidden. The  $C_{2v}$  point group imposed on the reacting system must be reduced to its three partial groups so as to find a likely elimination path. Figure 1 exhibits the three ways of symmetry relaxations. Among the three, the  $C_s$ -symmetry conserving path was found to be symmetry allowed. That is, a plane composed of two carbon and two nitrogen atoms should be a mirror plane throughout the reaction of eq 3.

The  $C_{2v} \rightarrow C_s$  symmetry lowering for the ready reaction initiation may be predicted by the second-order perturbation theory by Bader and MacDougall.<sup>20</sup> The theory states that the antisymmetric stretching vibration brings about the mixing with the lowest excited state and leads to the lowering of the energy barrier toward the geometric distortion. The favorable relaxation of the electron density through the vibrational mode corresponds to our symmetry lowering model.



**Figure 2.** CASSCF(2,2)/6-31G(d) geometries in eq 3. For TSs, sole imaginary frequencies corresponding to the reaction-coordinate vectors are shown. Geometric parameters (a–d) are shown in Table 1 along with those of CASSCF(4,4)/6-31G(d) and CASSCF(2,2)/6-311+G(d,p) calculations. Both TS1a and TS2a are not for  $5 \rightarrow 6$  isomerization but for the dissociation to the products. In square brackets, enthalpy and entropy changes are shown in kcal/mol and cal/(mol·K), respectively at  $T = 420$  K.

#### IV. Calculated Results of Geometries

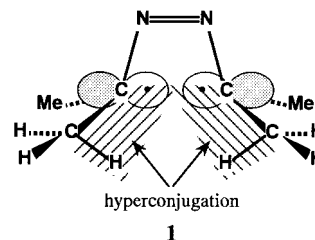
According to the prediction of the W–H rule,  $C_s$ -symmetry reaction routes in eq 3 were traced and are shown in Figure 2. The geometric parameters are shown in Table 1. As a result of calculations, any biradical intermediates (e.g., **7**) were not obtained. Also, the isomerization channel of  $5 \rightarrow 6$  was found to be absent. The diazetine **5** is decomposed concertedly. A striking result is that the transition state TS1a does not have the  $C_s$  symmetry. The  $C_s$ -symmetry constrained TS geometry, TS1a', was also obtained but has two imaginary frequencies, 342.2i and 217.5i  $\text{cm}^{-1}$ . One frequency corresponds to the expected C–N bond scission vibrational mode, and the other to the out-of-plane bending mode. Following the second mode, we obtained the correct TS, TS1a, with an imaginary frequency, 361.8i  $\text{cm}^{-1}$ . The  $C_s$  symmetry is slightly broken with the  $\angle\text{N–N–C–C}$  dihedral angle = 14.9° (Table 1). That is, the W–H rule is broken. On the other hand, the decomposition path of **6**, TS2a, has  $C_s$  symmetry, according to the W–H rule. TS1a and TS2a are of the strong biradical character with the natural orbital occupations, (1.5006, 0.4994) and (1.5325, 0.4675), respectively. The breakdown of the W–H rule for TS1a is a significant problem, and then further computational examinations were made. One is the set of active electrons and orbitals in the CASSCF space. CASSCF(4,4)/6-31G\* data are shown in Table 1. The other is the basis set dependence. CASSCF(2,2)/6-

311+G(2d,p) data are shown. Even by these examinations, the contrast between  $C_1$ -symmetry TS1a and  $C_s$ -symmetry TS2a was confirmed. In Figure 2, the energy of **6** is higher than that of TS1a, which demonstrates that the diazetine **5** decomposes to the product without the isomerization to **6**.

Figure 3 shows geometries concerned with eqs 1 and 2. The substituent effect of four methyl groups on those geometries was investigated. In TS1b, the  $\angle\text{N–N–C–C}$  dihedral angle is 19.5°, which shows again that the W–H rule is broken down. Geometries of TS1b and TS2b are close to those of TS1a and TS2a (Figure 2), respectively.

Energy and entropy changes are shown in square brackets of Figures 2 and 3. The experimentally available data are shown in eq 1. The calculated reaction energy  $\Delta H^\circ = -51.3$  kcal/mol (Figure 3) is in excellent agreement with the experimental one,  $-50.1$  kcal/mol.<sup>1</sup> The calculated activation enthalpy  $\Delta H^\ddagger = 35.3$  kcal/mol is slightly larger than the experimental one,  $\Delta H^\ddagger = 31.7 \pm 0.3$  kcal/mol.<sup>1</sup> The calculated activation entropy  $\Delta S^\ddagger = +0.94$  cal/(mol·K) is in fair agreement with the experimental one,  $\Delta S^\ddagger = 0.3 \pm 0.8$  cal/(mol·K).<sup>1</sup>

Energies in Figure 2 are compared with those in Figure 3. Methyl substituents were found to enlarge relative energies. That is, the tetramethyl-substituted diazetine **1** is more stable than



the parent one **5**. Diazetines have large instability of four-membered rings involving the N=N double bond. For the tetramethyl diazetine **1**, the ring strain is somewhat relaxed through the elongated C–C distance,  $d = 1.572$  Å (Figure 3). The elongation comes from the slight diffusion of the  $sp^3$   $\sigma$ -orbital component via hyperconjugation. The elongation has a negative effect on the C–C covalent bond but has a positive effect on the relaxation of the ring strain for stability. The C–C distance,  $d$ , is hardly affected by the computational methods,  $d = 1.572$  Å (1.538 Å) by CASSCF(2,2)/6-31G\*,  $d = 1.573$  Å (1.538 Å) by RHF/6-31G\*,  $d = 1.587$  Å (1.545 Å) by B3LYP/6-31G\*, and  $d = 1.571$  Å (1.537 Å) by MP2/6-31G\*. Here, distances in parentheses are of the parent diazetine, **5**. On the other hand, reaction energies (without thermal corrections) differ appreciably due to the opposing (negative and positive) effects. Those energies in kcal/mol are  $-48.3$  ( $-58.9$ ) by BCCD(T)/6-31G\*,  $-63.5$  ( $-67.6$ ) by RHF/6-31G\*,  $-49.4$  ( $-50.4$ ) by B3LYP/6-31G\*, and  $-51.8$  ( $-60.0$ ) by MP2/6-31G\*.

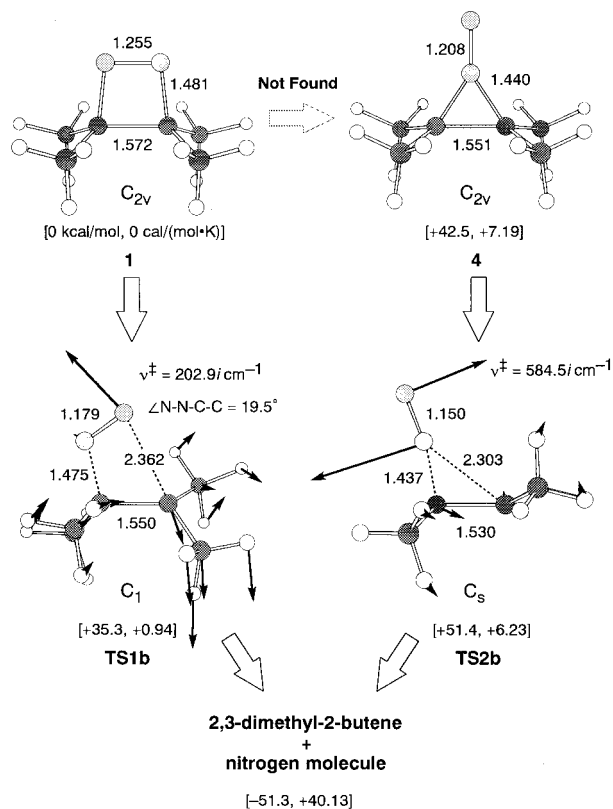
#### V. Discussions of the Orbital Mixing

In Figure 2, while TS2a has followed the symmetry conservation rule, TS1a has not done so. The contrast is examined here in terms of the orbital mixing rule.<sup>21</sup> Scheme 1 explains the contrast. In general, when two occupied orbitals ( $1a'$  and  $1a''$ , irreducible representations of  $C_s$  point group) mix with each other by symmetry relaxation, an energy splitting is brought about. The energy change  $\Delta E_b$  is larger than  $\Delta E_c$ . Therefore, in the framework of the one electron configuration (RHF method), the mixing of orbitals of different irreducible representations leads merely to instability of the system ( $\Delta E > 0$ , our RHF/6-31G\* calculation gives the TS with  $C_s$  symmetry

**TABLE 1: Geometric Parameters of the Parent System C<sub>2</sub>H<sub>4</sub>N<sub>2</sub> Shown in Figure 2**

method	class	species	<i>a</i> (C–N) <sup>a</sup>	<i>b</i> (N–N) <sup>a</sup>	<i>c</i> (C–N) <sup>a</sup>	<i>d</i> (C–C) <sup>a</sup>	∠N–N–C–C <sup>b</sup>
CAS(2,2)/6-31G*	reactant	diazetene <b>5</b>	1.471	1.229	1.471	1.538	
		isomer <b>6</b>	1.425	1.202	1.425	1.528	
	TS	TS1a	2.289	1.184	1.453	1.522	14.9
		TS1a'	2.385	1.182	1.453	1.527	0
		TS2a	2.279	1.146	1.418	1.502	0
CAS(4,4)/6-31G*	product	ethylene				1.317	
		N <sub>2</sub>		1.079			
		TS1a	2.348	1.208	1.456	1.517	18.0
CAS(2,2)/6-311+G(d,p)		TS2a	2.280	1.163	1.420	1.501	0
		TS1a	2.281	1.176	1.451	1.519	14.4
		TS2a	2.262	1.133	1.418	1.500	0

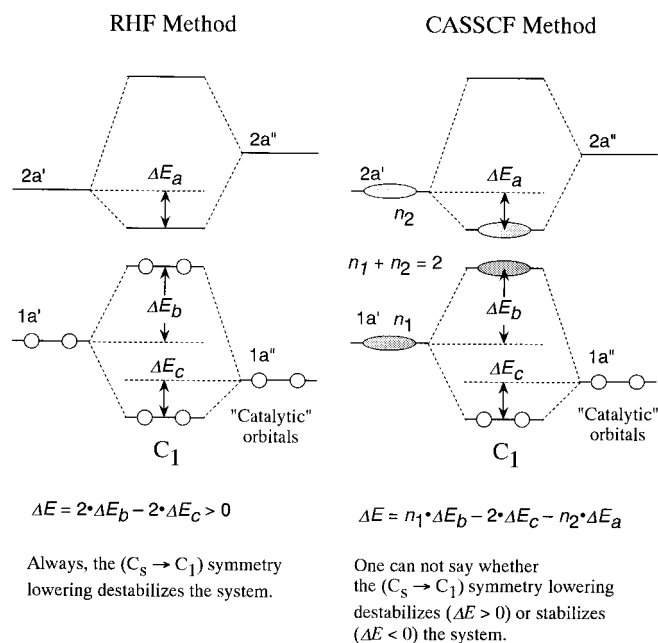
<sup>a</sup> *a*–*d* are in angstroms. <sup>b</sup> The dihedral angle ∠N–N–C–C is in degrees, and the zero value corresponds to C<sub>s</sub> symmetry.



**Figure 3.** CASSCF(2,2)/6-31G(d) geometries of tetramethyl-substituted diazetine (**1**), its isomer, and decomposition transition states, TS1b and TS2b. Distances are in angstroms.

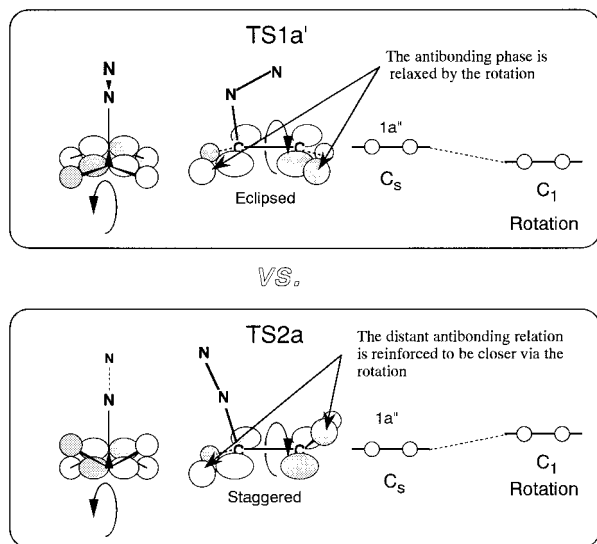
corresponding to TS1a'). The symmetry of the system tends to be conserved. However, when two electron configurations contribute to the electronic structure of the system, the orbital mixing rule must be extended to the following double mixing. By the "double mixing", both 1a'–1a'' and 2a'–2a'' interactions must be considered, while in the RHF model only the 1a'–1a'' one is treated. Two a' orbitals are natural orbitals, and their occupation numbers are not integers (total is 2). In fact, CASSCF(4,4)/6-31G\* occupation numbers in TS1a are 1a'' = 1.90, 1a' = 1.46, 2a' = 0.54, and 2a'' = 0.10, respectively. 1a'' and 2a'' are antisymmetric orbitals with respect to the molecular plane, and 1a' and 2a' are symmetric orbitals. 1a'' and 2a'' have C–H bonding and antibonding characters, respectively. 1a' and 2a' have C–N (breaking C–N) bonding and antibonding characters, respectively. Approximately, 1a'' and 2a'' are "catalytic" orbitals, and the electrons of the 1a' orbital flow out to the 2a' orbital at the transition state (the biradical character). In the "catalytic orbital", occupation numbers (1a'' = 1.90 and 2a'' = 0.10) are not so different from those (1a'' = 2 and 2a''

**SCHEME 1: (a'–a'') Orbital Mixing Caused by the (C<sub>s</sub> → C<sub>1</sub>) Symmetry Lowering, Which Leads Either to Stabilization (ΔE < 0) or to Destabilization (ΔE > 0)**



= 0) in the RHF model. As in the standard one-configuration case, the 1a'–1a'' mixing destabilizes the system. On the contrary, the 2a'–2a'' mixing stabilizes the system. Therefore, in biradical electronic states one cannot say generally that the a'–a'' Jahn–Teller type<sup>22</sup> mixing stabilizes or destabilizes the system. One criterion is the energy level of four orbitals. The larger 1a'–1a'' energy gap and the smaller 2a'–2a'' one leads to stabilization (vice versa). The other criterion is the extent of effective mixing spatially. Even if the 2a'–2a'' energy gap is small, large orbital components at the mixing point are required to stabilize the mixed orbital.

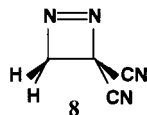
In the present case, another factor contributes to the a'–a'' Jahn–Teller type mixing. A remarkable difference between TS1a' and TS2a geometries is the position of two right-side methylene groups (see Figure 2). While the methylene groups in TS1a' are almost eclipsed (downward), they are staggered (upward) in TS2a. Now, let us consider the rotation of one methylene group (right-side in Figure 2) around the C–C bond. This rotation gives the symmetry relaxation. The 1a'' orbital is localized on the two methylene groups. The rotation from the staggered form (TS2a) raises the 1a'' orbital energy level, while that from the eclipsed form (TS1a') lowers the energy level as Scheme 2 shows. As the result, the 1a'–1a'' orbital mixing in TS1a' gives large ΔE<sub>c</sub> in Scheme 1, while that in TS2a does not so much.

**SCHEME 2: Changes of the 1a'' Orbital Energy Level Caused by the Rotation of the Methylene Group**


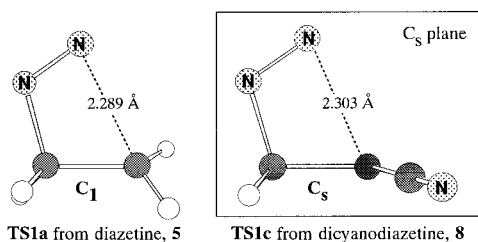
The orbital energy change caused by the rotation of the methylene group is examined by RHF/6-31G\* method using the TS1a' and TS2a geometries. The energy change,  $\Delta E$ , defined in Scheme 1 is also calculated. Table 2 shows the result. While the orbital energy of 1a'' in TS1a' is lowered markedly (0  $\rightarrow$  29  $\rightarrow$  116), that in TS2a is not done so much (0  $\rightarrow$  6  $\rightarrow$  19). The energy change  $\Delta E$  in TS1a' becomes negative (0  $\rightarrow$  -20.5  $\rightarrow$  -90.5) as the angle  $\theta$  is enlarged, which means the stabilization of the TS by the symmetry relaxation. However, that in TS2a is positive (0  $\rightarrow$  52.5  $\rightarrow$  214), and the methylene group rotation leads to destabilizing the system. That is, the geometry of TS2a is kept in  $C_s$  symmetry.

Both the 1a''-1a' and 2a'-2a'' orbital mixings are a kind of the geminal  $\sigma$  bond participations proposed by Inagaki et al.<sup>23</sup> They disclosed the significant participation of  $\sigma$  bonds geminal to the reacting center at the TSs. In the present system, 1a' and 2a' are the reacting-center orbitals, and 1a'' and 2a'' are the geminal  $\sigma$  bond orbitals. The symmetry relaxation causes the participation of the  $\sigma$  bond to the reacting center.

Now, we examine the geminal bond participation at the TS of the decomposition of a model diazetine, dicyanodiazetine, **8**. The orbital energy of the occupied geminal bonds (C-CN) is expected to be low and the geminal bond participation is



small. The TS search from **8** was carried out by the CAS(2,2)/6-31G\* method. The TS structure obtained, TS1c, has  $C_s$  symmetry as the following figure shows.

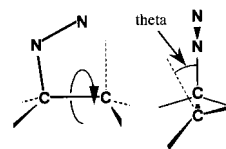


The energy change,  $\Delta E$ , of TS1c by the  $C_s \rightarrow C_1$  symmetry relaxation is also examined by the RHF/6-31G\* method as those

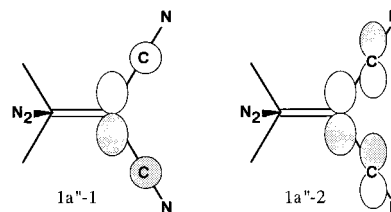
**TABLE 2: Changes ( $\Delta E_x$ ) of Orbital Energies by the Rotation of Methylene Group Calculated by the RHF/6-31G\* Method in au ( $\times 10^5$ )<sup>a,b</sup>**

(1) TS1a'			
orbital (occupation)	$\theta = 0^\circ$ (TS1a')	$\theta = 10^\circ$ ( $\Delta E_x$ )	$\theta = 20^\circ$ ( $\Delta E_x$ )
2a'' (0)	15 561	15 544	15 492
2a' ( $n_2 = 0.5$ ) <sup>c</sup>	3533	3467 (66)	3270 (263)
1a' ( $n_1 = 1.5$ ) <sup>c</sup>	-25918	-25871 (47)	-25736 (182)
1a'' (2)	-50441	-50470 (29)	-50557 (116)
$\Delta E^d$	0	-20.5	-90.5
(2) TS2a			
orbital (occupation)	$\theta = 0^\circ$ (TS2a)	$\theta = 10^\circ$ ( $\Delta E_x$ )	$\theta = 20^\circ$ ( $\Delta E_x$ )
2a'' (0)	8784	8739	8602
2a' ( $n_2 = 0.5$ ) <sup>c</sup>	7896	7839 (57)	7668 (228)
1a' ( $n_1 = 1.5$ ) <sup>c</sup>	-22591	-22529 (62)	-22347 (244)
1a'' (2)	-48720	-48726 (6)	-48739 (19)
$\Delta E^d$	0	52.5	214
(3) TS1c (Dicyanodiazetine)			
orbital (occupation)	$\theta = 0^\circ$ (TS)	$\theta = 10^\circ$ ( $\Delta E_x$ )	$\theta = 20^\circ$ ( $\Delta E_x$ )
2a'' (0)	5146	5073	4857
2a' ( $n_2 = 0.5$ ) <sup>c</sup>	-5014	-5070 (56)	-5233 (219)
1a' ( $n_1 = 1.5$ ) <sup>c</sup>	-32643	-32600 (43)	-32473 (170)
1a''-2 (2) <sup>e</sup>	-71150	-71138 (-12)	-71105 (-45)
1a''-1 (2) <sup>e</sup>	-80699	-80725 (26)	-80805 (106)
$\Delta E^d$	0	8.5	23.5

<sup>a</sup>  $\theta$  is the rotation angle around the olefinic C-C bond.  $0^\circ$  means the  $C_s$  symmetry of TS1a' and TS2a.



<sup>b</sup>  $\Delta E_x$  is the orbital energy difference between  $\theta = 0^\circ$  and  $\theta = 10^\circ$  and  $20^\circ$ . For instance, in the third and fourth columns of the upper table, (1) TS1a', (66) = 3533-3467 and (263) = 3533-3270. <sup>c</sup>  $n_1$  and  $n_2$  are assumed occupation numbers. <sup>d</sup>  $\Delta E$  is calculated by the equation in Scheme 1,  $\Delta E = n_1 \Delta E_b - 2 \Delta E_c - n_2 \Delta E_a$ . The negative value means the stabilization of the system. <sup>e</sup> In dicyanodiazetine, two a'' orbitals participate in the orbital mixing caused by the rotation.



of TS1a' and TS2a. The result is shown in Table 2. The dicyanodiazetine **8** has two occupied geminal bond orbitals, 1a''-1 and 1a''-2. 1a''-1 is the bonding orbital between the 2p orbital of the methylene carbon and the 2s orbital of the cyano carbon, and 1a''-2 is that between the 2p orbitals of the methylene and cyano carbons. The energy change is calculated by the following equation.

$$\Delta E = n_1 \Delta E_b(1a') - 2 \Delta E_c(1a''-1) - 2 \Delta E_c(1a''-2) - n_2 \Delta E_a$$

As the angle  $\theta$  is enlarged, the orbital energy of 1a''-1 is lowered (0  $\rightarrow$  26  $\rightarrow$  106), while that of 1a''-2 is raised (0  $\rightarrow$  -12  $\rightarrow$  -45). Totally, the 1a'' type orbitals, 1a''-1 and 1a''-2, do not contribute to the stabilization of TS1c effectively. As the result, the energy change  $\Delta E$  is positive (0  $\rightarrow$  8.5  $\rightarrow$  23.5). This energy increase means that the geometry of TS1c is kept

in  $C_s$  symmetry and the geminal bond participation is small. The reason for the small geminal bond participation is the large energy gap between  $1a''$  and  $1a'$  orbitals. In TS1a', the energy gap is  $24\,523 \times 10^{-5}$  au, while in TS1c, the gaps are  $48\,056 \times 10^{-5}$  [ $1a' - (1a''-1)$ ] and  $38\,507 \times 10^{-5}$  [ $1a' - (1a''-2)$ ] au.

## VI. Concluding Remarks.

In this work, decomposition paths of the smallest cyclic azoalkane, diazetine (**1** and **5**) and its isomer (**4** and **6**), have been investigated. Each species reacts independently to afford an olefin and a nitrogen molecule.  $C_{2v}$ -symmetry paths are symmetry forbidden, and  $C_s$ -symmetry paths become allowed through ( $a_1 + b_2 \rightarrow a'$ ) and ( $a_2 + b_1 \rightarrow a''$ ) orbital mixing. The isomer decomposition path (TS2a or TS2b) follows the W–H symmetry conservation rule, but the diazetine path (TS1a or TS1b) does not follow it. In the biradical TSs, dual orbital mixing takes place, which is beyond the W–H rule. The rule basically resorts to the one-configuration description. When multiple electron configurations are concerned with the orbital mixing, Jahn–Teller type geometric distortions may be brought about during the reaction.

**Acknowledgment.** The authors are grateful to Mr. S. Furukawa and Mr. S. Kawajiri for their assistance of the present calculations.

## References and Notes

- (1) Engel, P. S.; Hayes, R. A.; Keifer, L.; Szilagy, S.; Timberlake, J. W. *J. Am. Chem. Soc.* **1978**, *100*, 1876.
- (2) Greene, F. D.; Gilbert, K. E. *J. Org. Chem.* **1975**, *40*, 1409.
- (3) Freeman, J. P.; Graham, W. H. *J. Am. Chem. Soc.* **1967**, *89*, 1761.
- (4) Woodward, R. B.; Hoffmann, R. *The Conservation of Orbital Symmetry*; Verlag Chemie: New York, 1970.
- (5) Budzelaar, P. H. M.; Cremer, D.; Wallasch, M.; Würthwein, E.-U.; Schleyer, P. v. R. *J. Am. Chem. Soc.* **1987**, *109*, 6290.
- (6) (a) Baird, N. C. *Can. J. Chem.* **1979**, *57*, 98. (b) Kao, J.; Huang, T.-N. *J. Am. Chem. Soc.* **1979**, *101*, 5546. (c) Lin, R.; Cui, Q.; Dunn, K. M.; Morokuma, K. *J. Chem. Phys.* **1996**, *105*, 2333. (d) Lyons, B. A.; Pfeifer, J.; Peterson, T. H.; Carpenter, B. K. *J. Am. Chem. Soc.* **1993**, *115*, 2427. (e) Sorescu, D. C.; Thompson, D. L.; Raff, L. M. *J. Chem. Phys.* **1995**, *102*, 7910. (f) Yamamoto, N.; Olivucci, M.; Celani, P.; Bernardi, F.; Robb, M. A. *J. Am. Chem. Soc.* **1998**, *120*, 2391. (g) Reyes, M. B.; Carpenter, B. K. *J. Am. Chem. Soc.* **2000**, *122*, 10163.
- (7) (a) Jahn, H. A.; Teller, E. *Proc. R. Soc.* **1937**, *A161*, 220. (b) Jahn, H. A. *Proc. R. Soc.* **1938**, *A164*, 117. (c) Liehr, A. D. *Annu. Rev. Phys. Chem.* **1962**, *13*, 47.
- (8) (a) Labanowski, J. K.; Andzelm, J. W. *Density Functional Methods in Chemistry*; Springer-Verlag: Berlin, 1991. (b) Seminario, J. M.; Politzer, P. *Modern Density Functional Theory. A Tool for Chemistry*; Elsevier: Amsterdam, 1995. (c) Parr, R. G.; Yang, W. *Density Functional Theory of Atoms and Molecules*; Oxford University Press: New York, 1989.
- (9) (a) Lee, C.; Yang, W.; Parr, R. G. *Phys. Rev. B* **1988**, *37*, 785. (b) Becke, A. D. *Phys. Rev. A* **1988**, *38*, 3098. (c) Becke, A. D. *J. Chem. Phys.* **1993**, *98*, 1372.
- (10) (a) Schreiner, P. R. *J. Chem. Soc., Chem. Commun.* **1998**, 483. (b) Schreiner, P. R. *J. Am. Chem. Soc.* **1998**, *120*, 4184.
- (11) (a) Cramer, C. J.; Nash, J. J.; Squires, R. R. *Chem. Phys. Lett.* **1997**, *277*, 311. (b) Cramer, C. J. *J. Am. Chem. Soc.* **1998**, *120*, 6261. (c) Cramer, C. J.; Squires, R. R. *J. Phys. Chem. A* **1997**, *101*, 9191.
- (12) (a) Rudenberg, K.; Sundberg, K. *Quantum Science. Method and Structure*; Calais, J. C., Ed.; Plenum: New York, 1997. (b) Roos, B.; Taylor, P. R.; Siegbahn, P. E. *Chem. Phys.* **1980**, *48*, 157. (c) Hegarty, D.; Robb, M. A. *Mol. Phys.* **1975**, *38*, 1795. (d) Eade, R. H. E.; Robb, M. A. *Chem. Phys. Lett.* **1981**, *83*, 362.
- (13) Andersson, K.; Malmqvist, P.-Å.; Roos, B. O. *J. Chem. Phys.* **1992**, *96*, 1218.
- (14) Andersson, K.; Roos, B. O. *Int. J. Quantum Chem.* **1993**, *45*, 591.
- (15) Čárský, P. In *The Encyclopedia of Computational Chemistry*; Schleyer, P. v. R., Allinger, N. L., Clark, T., Gasteiger, J., Kollman, P. A., Schaefer, H. F., III, Schreiner, P. R., Eds.; John Wiley & Sons: Chichester, U.K., 1998; Configuration Interaction, pp 485–497.
- (16) Cizek, J. *Adv. Chem. Phys.* **1969**, *14*, 35.
- (17) (a) Brueckner, K. A. *Phys. Rev.* **1954**, *96*, 508. (b) Dykstra, C. E. *Chem. Phys. Lett.* **1977**, *45*, 466. (c) Handy, N. C.; Pople, J. A.; Head-Gordon, M.; Raghavachari, K.; Trucks, G. W. *Chem. Phys. Lett.* **1989**, *164*, 185.
- (18) Cramer, C. J. *J. Am. Chem. Soc.* **1998**, *120*, 6261.
- (19) Frisch, M. J.; Trucks, G. W.; Schlegel, H. B.; Gill, P. M. W.; Johnson, B. G.; Robb, M. A.; Cheeseman, J. R.; Keith, T.; Petersson, G. A.; Montgomery, J. A.; Raghavachari, K.; Al-Laham, M. A.; Zakrzewski, V. G.; Ortiz, J. V.; Foresman, J. B.; Cioslowski, J.; Stefanov, B. B.; Nanayakkara, A.; Challacombe, M.; Peng, C. Y.; Ayala, P. Y.; Chen, W.; Wong, M. W.; Andres, J. L.; Replogle, E. S.; Gomperts, R.; Martin, R. L.; Fox, D. J.; Binkley, J. S.; Defrees, D. J.; Baker, J.; Stewart, J. P.; Head-Gordon, M.; Gonzalez, C.; Pople, J. A. *Gaussian 94*, Rev. E.1; Gaussian, Inc.: Pittsburgh, PA, 1995.
- (20) (a) Bader, R. F. W. *Mol. Phys.* **1960**, *3*, 137. (b) Bader, R. F. W. *Can. J. Chem.* **1962**, *40*, 1164. (c) Bader, R. F. W.; MacDougall, P. J. *J. Am. Chem. Soc.* **1985**, *107*, 6788.
- (21) Inagaki, S.; Fujimoto, H.; Fukui, K. *J. Am. Chem. Soc.* **1976**, *98*, 4054.
- (22) The Jahn–Teller effect is extended to show that the symmetry lowering leads to stabilization of the reacting system. The Bader's perturbation theory,<sup>20</sup> which describes the vibrationally induced molecular deformation is similarly related to the Jahn–Teller effect.
- (23) (a) Inagaki, S.; Ikeda, H. *J. Org. Chem.* **1998**, *63*, 7820. (b) Ikeda, H.; Naruse, Y.; Inagaki, S. *Chem. Lett.* **1999**, 363. (c) Ikeda, H.; Ushioda, N.; Inagaki, S. *Chem. Lett.* **2001**, 166. (d) Ikeda, H.; Kato, T.; Inagaki, S. *Chem. Lett.* **2001**, 270.